Disclaimer

This note has not been internally reviewed by the DØ Collaboration. Results or plots contained in this note were only intended for internal documentation by the authors of the note and they are not approved as scientific results by either the authors or the DØ Collaboration. All approved scientific results of the DØ Collaboration have been published as internally reviewed Conference Notes or in peer reviewed journals.

Diphoton Production in $p\overline{p}$ Collisions at $\sqrt{s} = 1.8 \, \mathrm{TeV}$

John Womersley¹

Fermi National Accelerator Laboratory, Batavia, IL 60510

July 25, 1995.

We present results on the $\gamma\gamma$ cross section as a function of invariant mass and photon E_T . The next to leading order (NLO) QCD prediction is in good agreement with the data. The effect of invariant mass and diphoton balance cuts, which test the next-to-leading order contributions to the cross section, is investigated. We also compare the distribution of k_T between samples of diphotons and highly electromagnetic jets, and find that the NLO QCD prediction models the shape of the $\gamma\gamma$ k_T distribution quite well.

I. INTRODUCTION

Diphoton production at the Tevatron is of interest, firstly, as a test of QCD. Next to leading order predictions are available, and CDF have reported [1] a cross section ~ 3 times higher than expected (though more recent unpublished results [2] are lower). Secondly, it is a major irreducible background to Higgs discovery in the channel $H \to \gamma \gamma$ at the LHC. Thirdly it provides a way to test recent suggestions [3] that significant additional k_T (due to soft gluon radiation) needs to be added to perturbative QCD calculations in order to correctly model photon production.

This study uses 60 pb⁻¹ of data taken during Run IB with the EM2_GIS_GAM filter, which required 2 EM objects with $E_T > 12 \,\text{GeV}$ at Level 2.

II. DATA SELECTION

Events were required to have two photon candidates satisfying the following cuts:

- $E_T^1 > 20 \,\text{GeV}, E_T^2 > 18 \,\text{GeV};$
- \bullet Isolation with $E_T^{R=0.4}-E_T^{R=0.2}<2\,\mathrm{GeV};$
- EM fraction > 0.96;
- $|\eta| < 0.9$ and detector IETA ≤ 9 ;

 $^{^1}$ womersley@d0sft.fnal.gov, http://d0sgi0.fnal.gov/ \sim womersle/womersle

- H-matrix $\chi^2 < 100$;
- CCEM crack cut (10% of 2π excluded);
- · No track found in the road in front of the EM cluster.

The combined acceptance and efficiency of these cuts is estimated to be 0.28 ± 0.03 from plate level Monte Carlo simulations including noise and pileup effects [4]. This includes a detector acceptance 0.81 ± 0.01 , a combined trigger and cut efficiency of 0.64 ± 0.03 , and a probability that no track from the underlying event be found in the road of 0.925 ± 0.05 . (The latter is estimated from data by counting the number of tracks found in random roads in $Z \to ee$ events). This combined efficiency is lower than previous estimates [5]. It has fallen because of the use of plate-level, rather than mixture, Monte Carlo, and through the inclusion of noise and pileup effects. The efficiencies were checked against data using $Z \to ee$ events in the region $20 < p_T^e < 50$ and found to agree to within 4% [4]; this 4% is included in the error on the efficiency estimation.

In addition to the cuts outlined above, it was found necessary to impose an invariant mass requirement to remove $Z \to ee$ events where both electron tracks were lost because of tracking inefficiencies. (The number of observed events in the Z mass region is consistent with a tracking efficiency of about 0.9). Events with $80 < m_{\gamma\gamma} < 110 \,\text{GeV}$ were therefore excluded.

217 events remain after these selections.

A complementary sample of highly electromagnetic jets was selected from the same diphoton trigger and dataset. The EM jets were selected by requiring the same kinematic cuts as above, but:

- Anti-isolation with $E_T^{R=0.4} E_T^{R=0.2} \ge 2 \text{ GeV};$
- $EM1/E \ge 0.01$;
- EM fraction > 0.90;
- One or more of: EM fraction < 0.96, H-matrix $\chi^2 \ge 150$, or ≥ 2 tracks found in the road in front of the EM cluster.

These selections yield 81 events. This sample is expected to be composed almost entirely of dijet events where both jets have fragmented into electromagnetically-decaying particles. No real isolated photons are expected to remain in this sample.

III. BACKGROUND ESTIMATION

Even after the photon selection cuts described above, a significant background still remains from events where a jet has fragmented into a hard π^0 or η meson and which is found in the detector as a photon. The probability for this to occur in DØ is $\sim 5 \times 10^{-4}$, but since the QCD dijet cross section is a few $\times 10^6$ times higher than the $\gamma\gamma$ cross section, and the $\gamma + jet$ cross section is a few $\times 10^3$ times higher than the $\gamma\gamma$ cross section, both of these must be considered as potential sources of background.

The background estimation technique relies on the fraction of photon candidates having an energy in EM Layer 1 which is less than 1% of the shower energy (EM1/E < 0.01) as a discriminant. Real photons have a higher probability to have EM1/E < 0.01 than the multiphoton backgrounds from π^0 and η decays, because they are less likely to convert early. The EM1/E distribution has been shown to be stable between Run IA and Run IB. The probabilities ϵ_{γ} and $\epsilon_{\rm jet}$ for photons and electromagnetically-fragmenting jets, respectively, to have EM1/E < 0.01, are estimated from plate level Monte Carlo [4] (jets are treated as an admixture of π^0 and η mesons). Both ϵ_{γ} and $\epsilon_{\rm jet}$ depend upon the photon E_T , but given the very limited statistics, it is not possible to estimate the background as a function of E_T ; instead ϵ_{γ} and $\epsilon_{\rm jet}$ have been evaluated at $E_T = 29$ GeV, the mean E_T both of the photons in the signal sample and the jets in the background sample. Here $\epsilon_{\gamma} = 0.231$ and $\epsilon_{\rm jet} = 0.084$.

One may then write:

$$\begin{pmatrix} N_{PP} \\ N_{PF} \\ N_{FF} \end{pmatrix} = \begin{pmatrix} \epsilon_{\gamma}^{2} & \epsilon_{\gamma}\epsilon_{\rm jet} & \epsilon_{\rm jet}^{2} \\ 2\epsilon_{\gamma}(1-\epsilon_{\gamma}) & \epsilon_{\gamma}(1-\epsilon_{\rm jet}) + \epsilon_{\rm jet}(1-\epsilon_{\gamma}) & 2\epsilon_{\rm jet}(1-\epsilon_{\rm jet}) \\ (1-\epsilon_{\gamma})^{2} & (1-\epsilon_{\gamma})(1-\epsilon_{\rm jet}) & (1-\epsilon_{\rm jet})^{2} \end{pmatrix} \begin{pmatrix} N_{\gamma\gamma} \\ N_{\gamma j} \\ N_{jj} \end{pmatrix}$$
(1)

where (N_{PP}, N_{PF}, N_{FF}) are the numbers of events with (2,1,0) photons satisfying EM1/E < 0.01, and $(N_{\gamma\gamma}, N_{\gamma j}, N_{jj})$ are the numbers of events which are true diphotons, photon+jet and dijets. One may then obtain $(N_{\gamma\gamma}, N_{\gamma j}, N_{jj})$ by matrix inversion. For $(N_{PP}, N_{PF}, N_{FF}) = (7,49,161)$ this inversion predicts an unphysical solution (the number of $\gamma + jet$ events in the sample is negative). The unphysical solution probably reflects the rather large statistical uncertainties on the observed numbers of events, particularly N_{PP} .

We therefore introduce an additional constraint on the relative amount of the two backgrounds, $N_{\gamma j}/(N_{\gamma j}+N_{jj})$. The $\gamma+jet$ background may be estimated as $N_{\gamma j}=\mathcal{L}\sigma_{\gamma j}\times P$ where P is the probability for a jet to fluctuate into a photon candidate. Similarly, $N_{jj}=\mathcal{L}\sigma_{"\gamma"j}\times P$, where $\sigma_{"\gamma"j}$ is the cross section for fake photons. Then $N_{\gamma j}/(N_{\gamma j}+N_{jj})=\sigma_{\gamma j}/(\sigma_{\gamma j}+\sigma_{"\gamma"j})$. From the single inclusive photon analysis, this ratio is known; it is the purity of the photon candidate sample. For $E_T=29\,\mathrm{GeV}$, we find [4] $\sigma_{\gamma j}/(\sigma_{\gamma j}+\sigma_{"\gamma"j})=0.31\pm0.05$. With $N_{\gamma j}/(N_{\gamma j}+N_{jj})$ fixed to this value, the 3×3 matrix equation can be reduced to 2 equations in 2 unknowns and solved directly. The variable N_{PP} is not used in the solution (as it has the largest uncertainty). We obtain $f=0.268\pm0.15\pm0.025$, where the first error is statistical and the second reflects the uncertainty in $N_{\gamma j}/(N_{\gamma j}+N_{jj})$. The inverted equations predict $N_{PP}=4$, which is in reasonable agreement with the observed value.

In order to estimate the systematic error that may arise from estimating the background using ϵ_{γ} and $\epsilon_{\rm jet}$ values which are constant rather than varying with E_T , ϵ_{γ} and $\epsilon_{\rm jet}$ were varied in a correlated way by amounts corresponding to $\pm 1\sigma$ in the E_T distribution. This results in an additional error of (+0.17, -0.14) on the $\gamma\gamma$ signal purity.

The effects of multiple interactions were checked by requiring the multiple interaction flag to be 2 or less, thus selecting predominantly single interaction events. Out of the 217 candidate events, 88 survive; the signal purity obtained for these events is $f = 0.45 \pm 0.24$. This suffers from loss of statistics but is completely consistent with the full sample, and so there is no indication that multiple interactions are biasing the signal purity estimate.

The systematic errors on the cross section have been combined in quadrature. They include $\pm 9.6\%$ from acceptance and efficiency, $\pm 5\%$ luminosity uncertainty, $\pm 56\%$ statistical error on the background subtraction, (+63%, -52%) systematic error on the background subtraction from varying E_T and $\pm 9.3\%$ from varying $N_{\gamma j}/(N_{\gamma j}+N_{jj})$. The combined error is (+85%, -75%).

The background subtraction has been carried out by multiplying the $\gamma\gamma$ candidate distribution by the signal purity. This is justified by the observation that the $\gamma\gamma$ candidates and the EM jet sample have very similar invariant mass and p_T distributions, so the background contribution to all bins is expected to be similar.

IV. DIPHOTON CROSS SECTION $D\sigma/DM_{\gamma\gamma}$

Fig. 1 shows the differential diphoton cross section $d\sigma/dm_{\gamma\gamma}$ as a function of the diphoton invariant mass $m_{\gamma\gamma}$. The data are compared with a next-to-leading order (NLO) QCD prediction [6], evaluated at a renormalization scale $\mu=E_T$ with CTEQ3M parton distributions; the data and theory are in good agreement over the whole range of invariant mass.

V. DIPHOTON CROSS SECTION $D\sigma/DE_T^{\gamma}$

Fig. 2 shows the differential diphoton cross section $d\sigma\epsilon/dE_T^{\gamma}$ as a function of the photon transverse energy E_T^{γ} (two entries per event). The dip in the cross section around $E_T^{\gamma}=50\,\mathrm{GeV}$ is due to the invariant mass cut applied

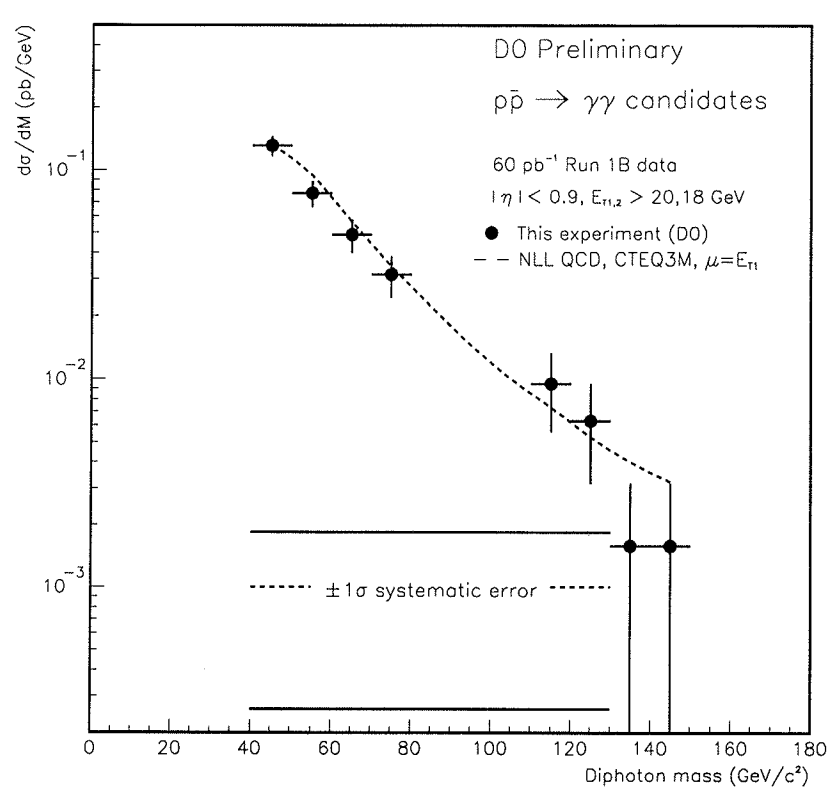


FIG. 1. Diphoton differential cross section $d\sigma/dm_{\gamma\gamma}$ as a function of the diphoton invariant mass $m_{\gamma\gamma}$. The plot contains 217 candidate events with an expected purity of 0.27.

18/07/95 17.00

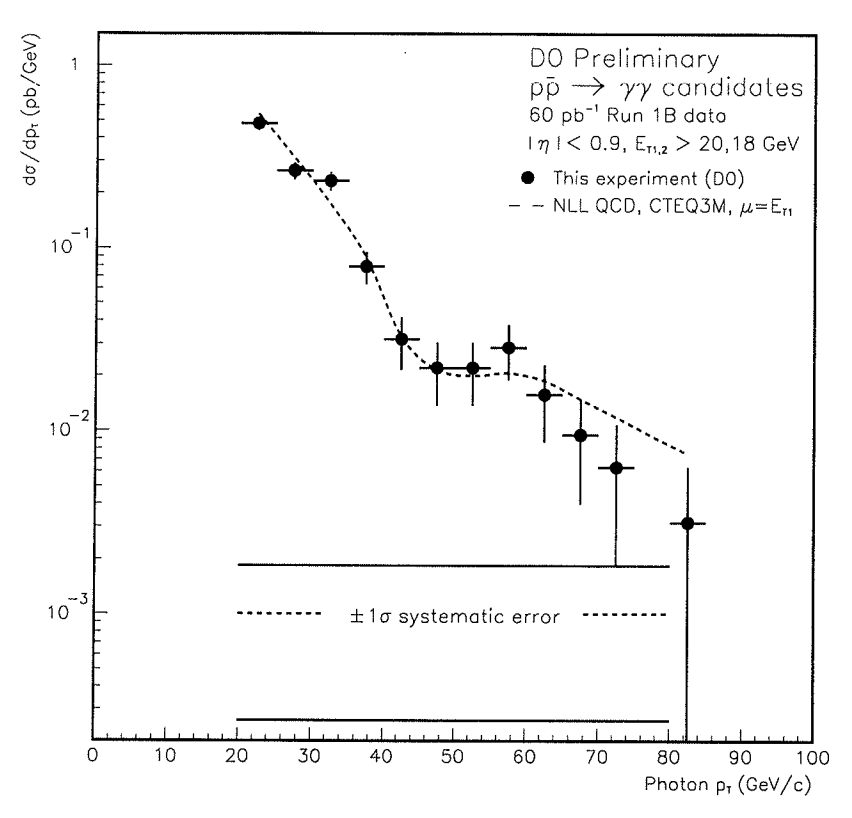
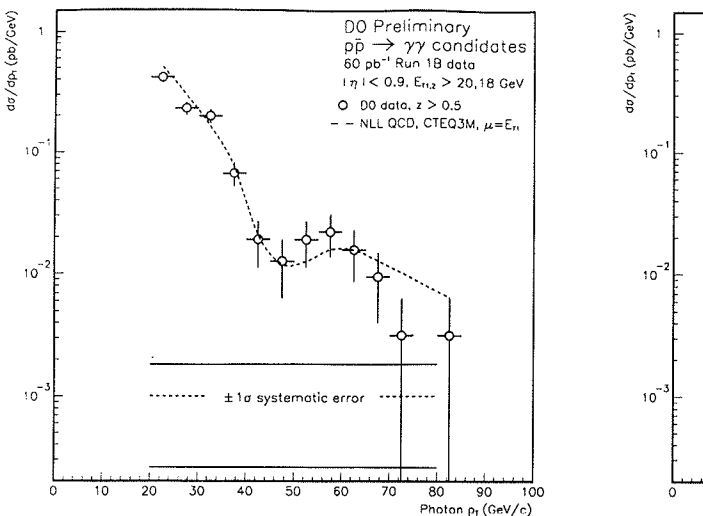


FIG. 2. Diphoton differential cross section $d\sigma\epsilon/dE_T^{\gamma}$ as a function of the photon transverse momentum E_T^{γ} . The probability to pass the invariant mass cut, ϵ , has not been corrected for. The plot contains 217 candidate events with an expected purity of 0.27.

18/07/95 17.00



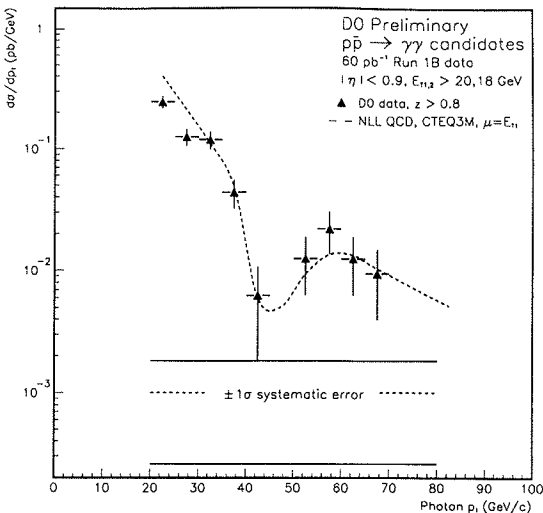


FIG. 3. Diphoton differential cross section $d\sigma\epsilon/dE_T^{\gamma}$ as a function of the photon transverse momentum E_T^{γ} , for imbalance cuts of (a) $z \ge 0.5$ and (b) $z \ge 0.8$. The probability to pass the invariant mass cut, ϵ , has not been corrected for.

to remove Z events; the probability to pass this cut (ϵ) has not been corrected for. The data are again compared with the next-to-leading order QCD prediction [6], and the agreement between data and theory is once again good, even in the region affected by the invariant mass cut. It is interesting to note that at leading order, there would be no events at all in this region, since the whole leading order cross section is due to back-to-back photon pairs. The population of events here is then a test of the next to leading order contributions to the QCD cross section. We may explore this effect further by introducing a cut on the imbalance between the two photons, z:

$$z = \frac{|\mathbf{p}_1 \cdot \mathbf{p}_2|}{\mathbf{p}_1^2} \tag{2}$$

where p_1 and p_2 are the vector momenta of the two photons. Requiring $z \ge 0.5$ or $z \ge 0.8$ selects events with increasingly back-to-back topologies, and correspondingly restricts the cross section to its leading order part, as can be seen in Fig. 3. The NLO QCD prediction remains in good agreement with the data for both of these cases.

VI. DIPHOTON K_T

We define the diphoton k_T by:

$$k_T = |\mathbf{p}_T^1 + \mathbf{p}_T^2| \tag{3}$$

where \mathbf{p}_T^1 and \mathbf{p}_T^2 are the vector transverse momenta of the two photons. Because $k_T \ll p_T^{1,2}$, it is not amenable to perturbative calculation, and ad hoc models of soft gluon radiation have been proposed to predict the distribution.

If soft gluon radiation is indeed important, then we may expect that the k_T distribution will be broader for dijet events (predominantly $gg \to gg$ scattering at the Tevatron) than for diphotons. This is because the probability for radiation is higher off gluon lines, and final state radiation can also contribute in this case.

Because we wish to investigate differences between the k_T distributions for diphoton and dijet events, it is desirable to use the purest possible $\gamma\gamma$ sample, and so an additional requirement was made: that one or both photons have EM1/E < 0.01. This results in 57 events with an estimated purity of 0.41. This enriched $\gamma\gamma$ sample

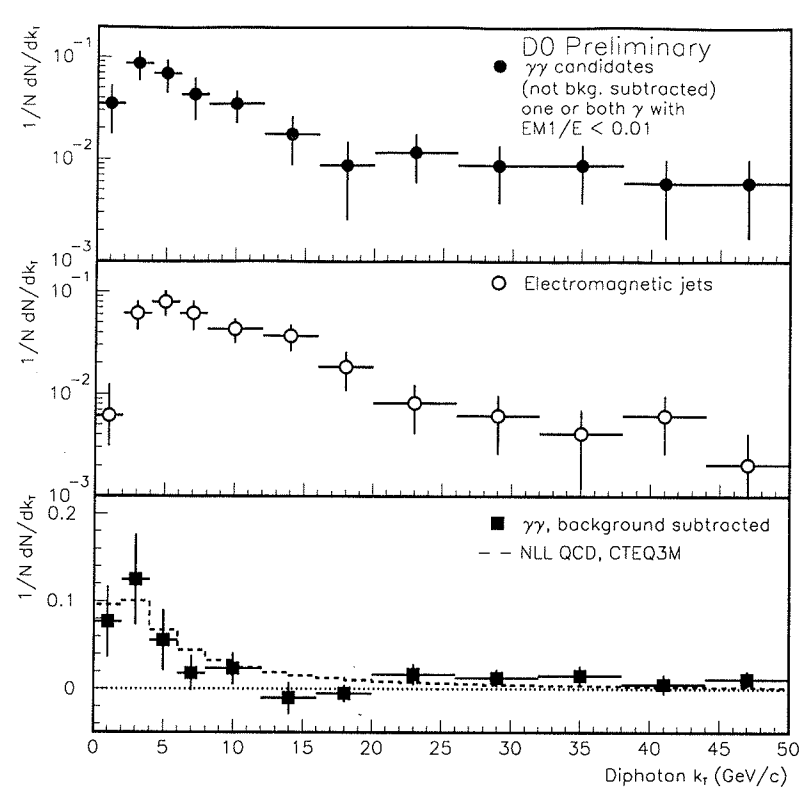


FIG. 4. Normalized differential k_T distributions, $1/NdN/dk_T$, for (a) an enriched sample of $\gamma\gamma$ candidates (56 events with a purity of 0.41), (b) highly electromagnetic jets (81 events), and (c) the $\gamma\gamma$ sample after subtraction of the background distribution.

will be compared with the EM jet sample. Since the purity of the signal sample is known, the background sample may be directly subtracted to yield a background-subtracted $\gamma\gamma$ distribution. (This assumes, of course, that the k_T of the $\gamma + jet$ and dijet contributions to the background are similar).

The normalized k_T distributions $1/N \, dN/dk_T$ for the three cases are shown in Fig. 4. While the general shape of both the diphoton and dijet distributions is similar, the dijet sample has a higher mean and most probable k_T (the fraction of events with $k_T < 4 \, \text{GeV}$ is $25 \pm 6\%$ for the diphotons and $14 \pm 4\%$ for the dijets). However, it must be noted that the EM jet selection permits more hadronic energy in the clusters than for the photon cuts, so the dijet events will have a worse energy resolution. A simple estimate suggests that for $p_T = 30 \, \text{GeV}$ candidates at $\eta = 0$, the k_T resolution is $\sim 1.2 \, \text{GeV}$ for diphotons and $\sim 1.7 \, \text{GeV}$ for EM jets. This could account for some or all of the difference in k_T distributions; more detailed modelling will be required to fully understand the magnitude of this effect. We cannot therefore claim at this time that the observed difference in k_T between diphotons and dijets has its origin in physics rather than detector effects.

The NLO QCD prediction [6] is shown superimposed on the the background-subtracted $\gamma\gamma$ distribution. The theory Monte Carlo included smearing the photon 4-vectors according to the $0.15\sqrt{E}$ energy resolution of the DØ calorimeter. The NLO QCD prediction models the k_T distribution quite well, even though it has been claimed that perturbative QCD should not be able to match the low- k_T behavior (below about 5 GeV) correctly.

VII. CONCLUSIONS

Results have been shown for the $\gamma\gamma$ cross section as a function of invariant mass and photon E_T . The next to leading order QCD prediction is in good agreement with the data. It is also able to correctly model the effect of the invariant mass and z cuts imposed on the data, which test the next-to-leading order contributions to the cross section.

The distribution of k_T has been compared between a sample of diphoton candidates and highly electromagnetic jets. The two distributions are generally similar, but the jet sample has a higher mean and most probable k_T . This may merely indicate the effects of worse energy resolution. A background-subtracted diphoton sample is compared with the NLO QCD prediction for k_T . The theoretical prediction matches the observed distribution quite well, although it is not expected to model the data below $k_T \sim 5 \, \text{GeV}$.

REFERENCES

- 1. CDF Collaboration, Phys. Rev. Lett. 70, 2232.
- 2. R. Blair, at the 10th Topical Workshop on $p\bar{p}$ Collider Physics, Fermilab, May 1995.
- 3. J. Huston et al., 'A Global Study of Direct Photon Production,' MSU-HEP-41027, CTEQ-407, January 1995.
- 4. S. Fahey, Ph.D. Thesis, Michigan State University, July 1995.
- 5. R. Madden, private communication.
- 6. B. Bailey, private communications.